A Single-Stage AC-AC HB Inverter with Boosting Stage for Induction Heating Applications

Bhavin Salvi
Department of Electrical Engineering
National Institute of Technology
Warangal, India
sbhavin@student.nitw.ac.in

S Porpandiselvi
Department of Electrical Engineering
National Institute of Technology
Warangal, India
selvi@nitw.ac.in

N Vishwanathan
Department of Electrical Engineering
National Institute of Technology
Warangal, India
nvn@nitw.ac.in

***Abstract*—Induction heating (IH) technology has gained attention of the heating appliance market due its several advantages over conventional heating technologies. Traditional IH solutions comprise of separate rectification and high frequency inversion stages. Efficiency of the IH system reduces due to more conversion stages. This paper proposes a single-stage ac-ac inverter with boosting stage. Rectification, voltage boosting and power control are done using three MOSFETs which reduces the component count. Duty cycle control is used for controlling IH load power. Provision of independent voltage boosting in positive and negative half cycle of the supply mains helps in maintaining good input current profile with simple control. The proposed ac-ac inverter offers a compact, efficient and cost-effective inverter configuration for IH applications. The operation of the proposed inverter is verified using MATLAB/Simulink software.**

Keywords—induction heating, reduced component count, acac inverter, duty cycle control, half bridge series resonant inverter (HB-SRI)

I. Introduction

Induction heating systems have become more popular in the market nowadays. It is majorly due to the advantages over conventional heating systems. IH systems offer clean and safe solution with high efficiency and better power control which is highly desirable.

Traditional IH solutions comprise of a diode bridge rectifier, filter capacitor and DC-AC inverter. Due to two stages of power conversions namely low frequency AC to DC and then DC to high frequency AC [1]–[3], losses are more in these solutions. In order to overcome this, single stage ac-ac solutions have been proposed in the literature [4]–[9].

Four quadrant switch approach is used for direct ac-ac conversion in [10], [11]. These configurations offer reliable solutions but suffer with more component count and complex control. Two diode rectification approach is used in [12], [13]. Half-bridge and quasi resonant configuration is combined for powering multiple IH loads in [14]. In [15], a boost half-bridge (HB) inverter is proposed. Boosting and HB-SRI operation is combined using an inverter leg which reduced the component count. However, control becomes more complex to obtain same boosting during positive and negative half cycle of the ac supply.

In this paper, a direct boost ac-ac inverter with reduced component count is proposed. The proposed converter uses two active switches for rectification as well as boosting operation. Due to reduced component count, the size and cost of the proposed ac-ac inverter is reduced. It also makes the converter more efficient. The proposed ac-ac inverter uses simple duty cycle control in order to regulate output power in IH load. Independent control in boost operation in each half cycle makes it easy to maintain a good input current profile of the ac mains. This paper is structured as follows. Section II describes the proposed ac-ac inverter and its modes of operation. Proposed inverter topology analysis is done in section III. Simulation results are presented in section IV. The major conclusions are included in section V.

II. Proposed AC-AC Boost Inverter

Circuit diagram of the proposed ac-ac boost inverter is as shown in Fig. 1. It consists of three switches, two capacitors and an induction heating load. The IH load is modelled as series combination of R_L-L_r. Capacitor C_r is used to resonate the IH load at resonant frequency $f_r = 1/2\pi\sqrt{L_r C_r}$ The MOSFET S_p, inductor L_s and capacitor C_{p1} form a boost circuit. It operates during positive half-cycle of utility voltage. MOSFET S_n, inductor L_s and capacitor C_{n1} also form a boost circuit and operate over negative half-cycle of voltage. The output voltage during positive input cycle can be controlled by duty cycle of S_p. The output voltage during negative input cycle can be controlled by S_n duty cycle. The switch S_z is used to get zero voltage state across the IH load. The combined operation of S_p and S_z is used to control the power in IH load during positive half cycle. The power control in IH load during negative half cycle is obtained by switches S_n and S_z. Fig. 2 shows the switching pulses and different modes of operations of the proposed inverter.

A. Switching strategy

The switching pattern of the devices is shown in Fig. 2(c). As shown in Fig. 2(a), switch S_p is conducting during positive polarity of the AC supply. S_n is conducting when supply voltage is negative. The duty cycle of S_p is d_p and that of S_n is d_n. The total time period for S_p is T_p and that of S_n is T_n. The switch S_z conducts during the entire cycle. The gate pulses of S_z during positive half cycle is complement to that of the S_p. The gate pulses of S_z during negative half cycle is complement to that of the S_n. The switching frequency f_s for S_p, S_n and S_z is selected a little higher to that of the

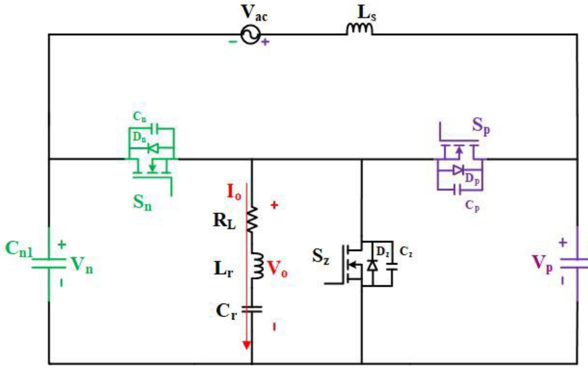

Fig. 1. Proposed single-stage AC-AC HB inverter.

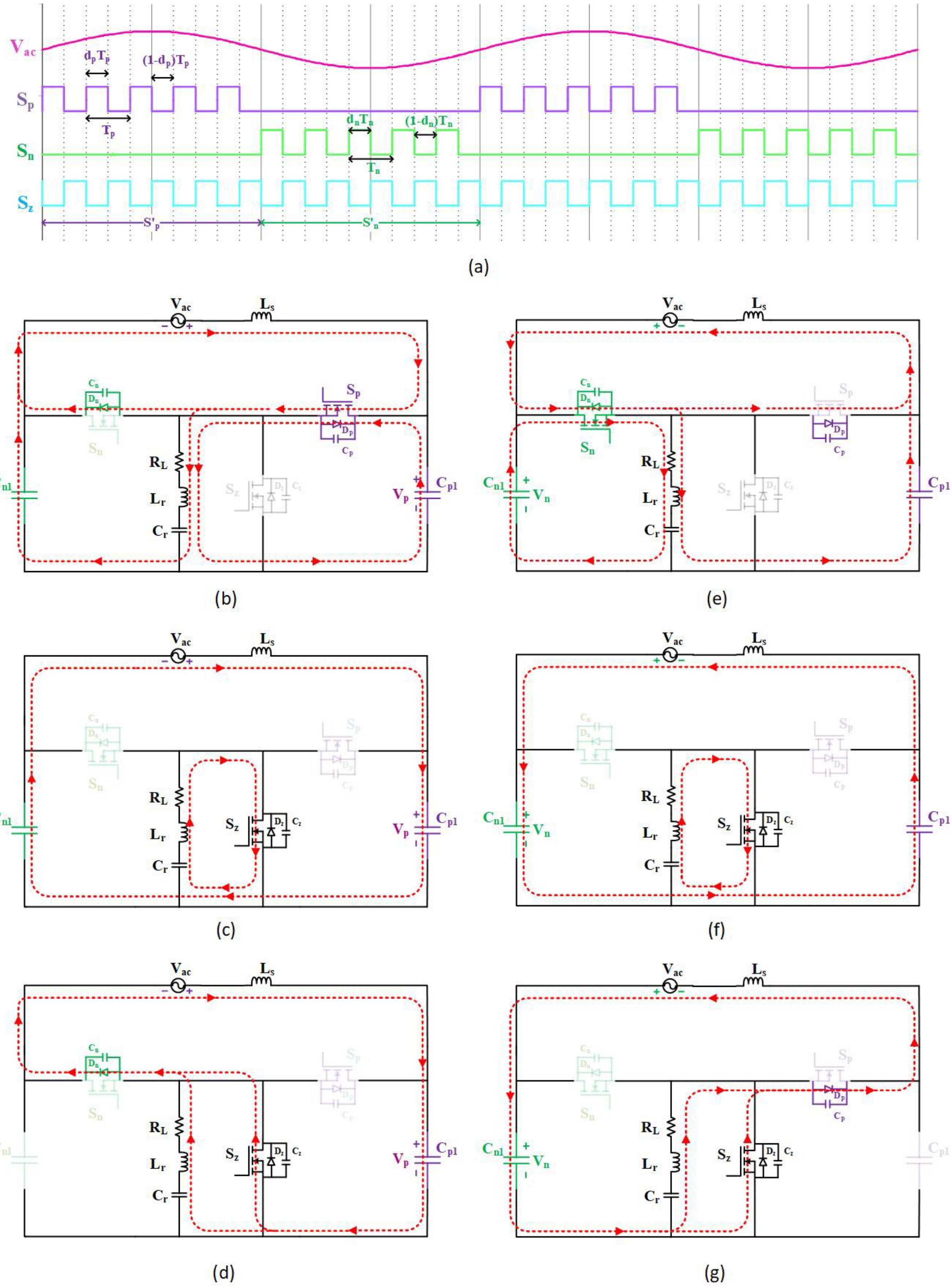

Fig. 2. Switching strategy and operating modes, (a) switching pulses, (b) Mode-I: positive half cycle and S_p ON, (c) Mode-II: positive half cycle and S_p OFF during $t_{p_{off1}}$, (d) Mode-III: positive half cycle and S_p OFF during $t_{p_{off2}}$, (e) Mode-IV: negative half cycle and S_n ON, (f) Mode-V: negative half cycle and S_n OFF during $t_{n_{off1}}$, (g) Mode-VI: negative half cycle and S_n OFF during $t_{n_{off2}}$.

resonant frequency f_r. Inverter operation during positive half-cycle follows operating modes I, II and III. Negative half-cycle inverter operation is described through modes IV, V and VI.

B. Mode-I: ($t_{p_{on}}$)

In this mode, ON time of the switch S_p, $t_{p_{on}}$ is considered. V_{ac} is positive. Operation of the proposed inverter during this mode is as per Fig. 2(b). The switch S_p is ON and S_z is OFF. The inductor L_s is charged from ac mains. The input current flows through L_s, S_p and D_n. The capacitor C_{n1} is discharged through the IH load via ac mains. The capacitor C_{p1} powers the IH load through switch S_p.

C. Mode-II: ($t_{p_{off\,1}}$)

This mode represents the operation of the circuit during some portion of OFF time period of S_p, $t_{p_{off\,1}}$. Inverter operation is depicted in Fig. 2(c). V_{ac} is positive. The switch S_p is OFF and S_z is ON. The inductor L_s is discharged through capacitor C_{n1} and C_{p1}. The current flows through L_s, C_{n1}, and C_{p1}. The capacitor C_{n1} gets charged in this mode. The load current freewheels through switch S_z.

D. Mode-III: ($t_{p_{off\,2}}$)

The operation during mode-III is as per Fig. 2(d). V_{ac} is positive. The switch S_p is OFF and S_z is ON. This mode represents the operation of the circuit during some portion of OFF time period of S_p, $t_{p_{off2}}$. The inductor L_s is discharged through capacitor C_{p1} and switch S_z. The current flows through L_s, C_{p1}, S_z and D_n. The capacitor C_{p1} gets charged in this mode. The load current freewheels through D_n, L_s and C_{p1}.

E. Mode-IV: ($t_{n_{on}}$)

In this mode, the switch S_n is ON for the duration of $t_{n_{on}}$. V_{ac} is negative. The inverter operation is as shown in Fig. 2(e). The switch S_n is ON and S_z is OFF. The inductor L_s is charged from ac mains. The input current flows through L_s, S_n and D_p. The capacitor C_{p1} is discharged through the IH load via ac mains. The capacitor C_{n1} discharges and powers the IH load through switch S_n.

F. Mode-V: ($t_{n_{off1}}$)

During this mode, the inverter operation is as per Fig. 2(f). V_{ac} is negative. The switch S_n is OFF and S_z is ON. This mode represents the operation of the circuit during some portion of the OFF time period of S_n, $t_{n_{off1}}$ The inductor L_s is discharged through capacitor C_{p1} and C_{n1}. The current flows through L_s, C_{p1}, and C_{n1}. The capacitor C_{p1} gets charged in this mode. The load current freewheels through switch S_z.

G. Mode-VI: ($t_{n_{off2}}$)

This mode represents the operation of the circuit during some portion of the OFF time period of S_n, $t_{n_{off2}}$ .Inverter operation is depicted in Fig. 2(g). V_{ac} is negative. The switch S_n is OFF and S_z is ON. The inductor L_s is discharged through capacitor C_{n1} and switch S_z. The current flows through L_s, C_{n1}, S_z and D_p. The capacitor C_{n1} gets charged in this mode. The load current freewheels through D_p, L_s and C_{n1}.

III. Inverter Analysis

The proposed inverter provides boosting operation for the voltage across capacitors C_{p1} and C_{n1} during positive and negative half cycles of the ac supply V_{ac} respectively. The IH load is powered in the same way as that of half bridge series resonant inverter (HB-SRI). The proposed inverter can be analysed by combining the boosting and HB-SRI operation together.

A. Boosting Operation

During positive half cycle, the volt-sec balance across an inductor L_s in steady state can be expressed as

$$V_{ac}t_{p_{on}} - V_n t_{p_{off}} + (V_{ac} - V_p + V_n)t_{p_{off1}} + (V_{ac} - V_p)t_{p_{off2}} = 0 \quad (1)$$

The voltage across C_{p1} can be expressed as

$$V_p = \frac{V_{ac}}{1-d_p} - \frac{V_n}{1-d_p} + \frac{V_n(2t_{p_{off1}} + t_{p_{off2}})}{t_{p_{off}}} \quad (2)$$

During negative half cycle, by using volt-sec balance across an inductor L_s in steady state, the voltage across C_{n1} can be expressed as

$$V_n = \frac{V_{ac}}{1-d_n} - \frac{V_p}{1-d_n} + \frac{V_p(2t_{n_{off1}} + t_{n_{off2}})}{t_{n_{off}}} \quad (3)$$

B. HB-SRI

The equivalent HB-SRI for the proposed inverter is powered by C_{p1} during positive half cycles and C_{n1} during negative half cycles. The output power of HB-SRI is described in [15]. Total output power during full-cycle can be written as

$$P_o = \sum_{n=0}^{\infty}\left[\frac{1-\cos(2\pi n d_p)}{(n\pi)^2}V_p^2 + \frac{1-\cos(2\pi n d_n)}{(n\pi)^2}V_n^2\right] * \frac{R_L}{R_L^2 + (2\pi f_s n L_r - \frac{1}{2\pi f_s n C_r})^2} \quad (4)$$

where n is the order of the harmonic. In order to obtain better input current profile, duty cycle d_p and d_n are kept same.

IV. Simulation Results

Simulation of the proposed ac-ac inverter configuration is performed in Matlab-Simulink environment for the parameters mentioned in Table I. Iron vessel material IH load is used in the proposed inverter. The IH load is resonated at $f_r = 28.376$ kHz. The switching frequency for all the three switches is selected as f_s = 30 kHz. The control over output power is obtained by varying duty cycles d_p and d_n during positive and negative half cycle of input supply respectively. The duty cycles d_p and d_n are kept equal to ensure better input current profile.

TABLE I. Circuit Parameters of the Proposed Inverter Configuration

Parameter	Value
source voltage, V_{ac}	230 V
filter inductor, L_s	500 μH
capacitors, $C_{p1} = C_{n1}$	1 μF
IH load equivalent resistance, R_L	6.5 Ω
IH load equivalent inductance, L_r	67 μH
resonant capacitor of IH load, C_r	0.47 μH
switching frequency, f_s	30 kHz
quality factor of IH load, Q	1.8

Simulation results at 20% duty cycle of the proposed ac-ac inverter are shown in Fig. 3. The IH load power is 582.92 W. Source voltage and current waveforms are shown in Fig. 3(a). The total harmonic distortion (THD) for the input current waveform is 8.17%. Fig. 3(b) depicts the output voltage waveform across the IH load. Fig. 3(c) shows the waveform for the current flowing through the load. Current of 9.47 A is flowing through the load.

Fig. 4 shows the simulation results for 60% duty cycle. The IH load is powered at 3997.76 W. Fig. 4(a) presents the source voltage and current waveforms. The THD for the input current waveform is 5.74%. Fig. 4(b) depicts the load voltage waveform. Fig. 4(c) shows the load current waveform. Current of 24.8 A flows through the load. Fig. 5 presents zoomed view of output voltage, output current, load voltage and load current waveforms. Fig. 6 shows the simulation results for 40% duty cycle. The IH load is powered at 1856.46 W. Fig. 6(a) depicts the source voltage and current waveforms. The THD for the input current waveform is 8.74%. Fig. 6(b) depicts the load voltage waveform. Fig. 6(c) shows the waveform of the current flowing through the load. Current of 16.9 A flows through the load.

The inverter performance is described in Table II with regards to input current profile for different output power. The proposed ac-ac inverter exhibits satisfactory performance over

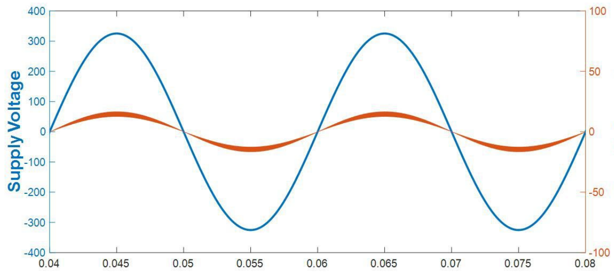

(a)

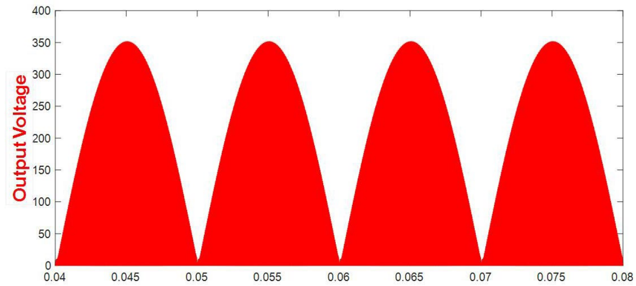

(b)

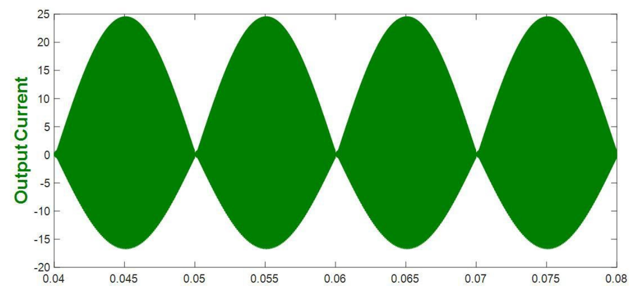

(c)

Fig. 3. Simulation results for IH load powered at 582.92 W, (a) supply voltage and supply current, (b) load voltage, V_o, (c) load current, I_o.

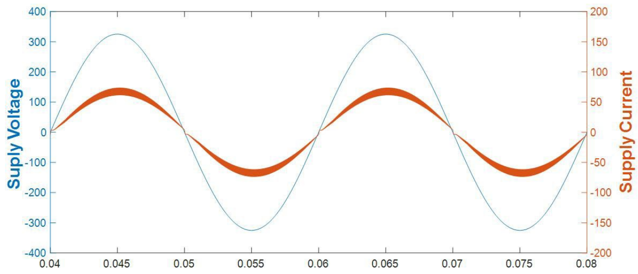

(a)

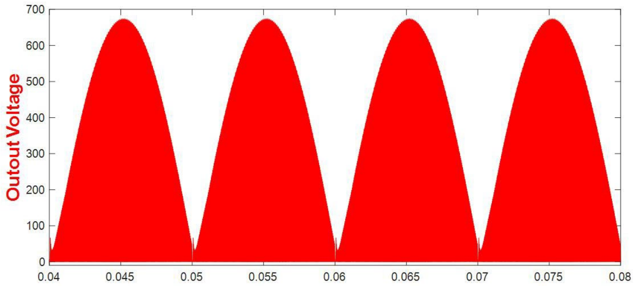

(b)

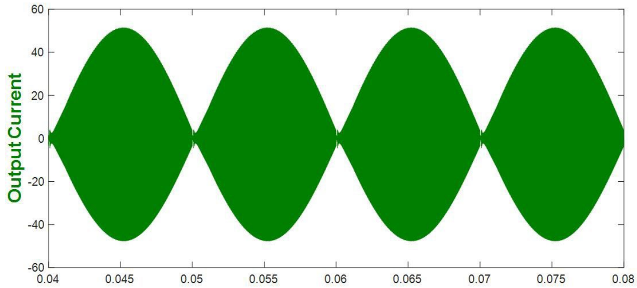

(c)

Fig. 4. Simulation results for IH load powered at 3997.76 W (a) supply voltage and supply current, (b) load voltage, V_o, (c) load current, I_o.

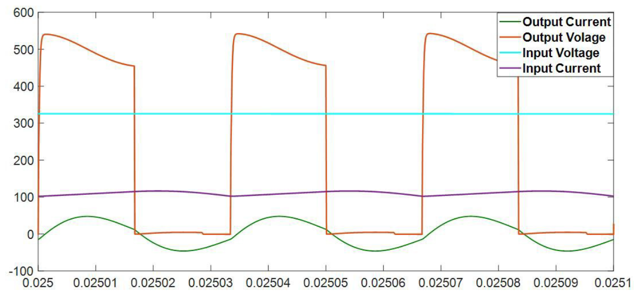

Fig. 5. Zoomed view of output current, output voltage, input voltage and input current waveform.

TABLE II. PERFORMANCE OF THE PROPOSED AC-AC INVERTER

Output Power	THD(%)
582.92 W	8.17
1856.46 W	8.74
2785.18 W	7.33
3997.76 W	5.74

the whole range of the output power. Variation of the load power with respect to duty cycle is depicted in Fig. 7.

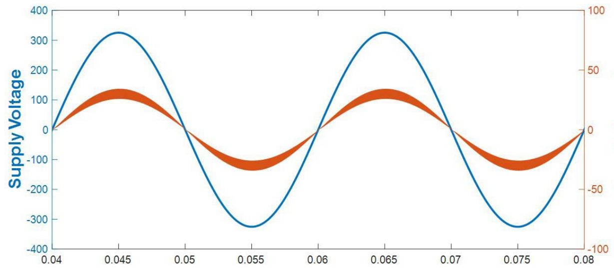

(a)

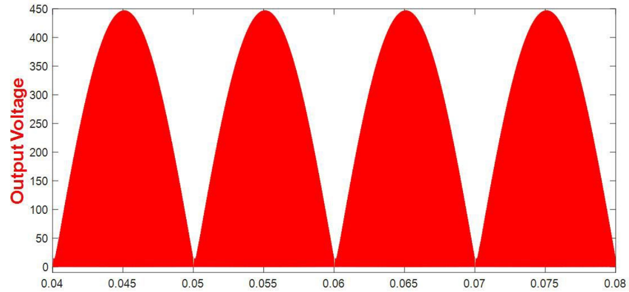

(b)

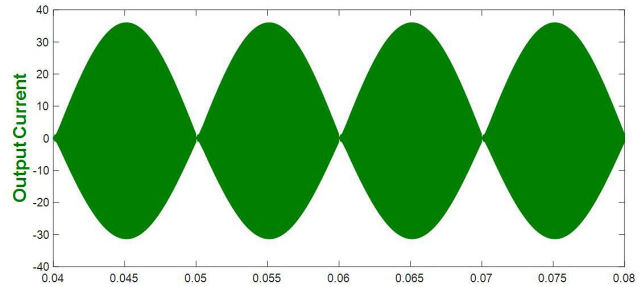

(c)

Fig. 6. Simulation results for IH load powered at 1856.46 W (a) supply voltage and supply current, (b) load voltage, V_o, (c) load current, I_o.

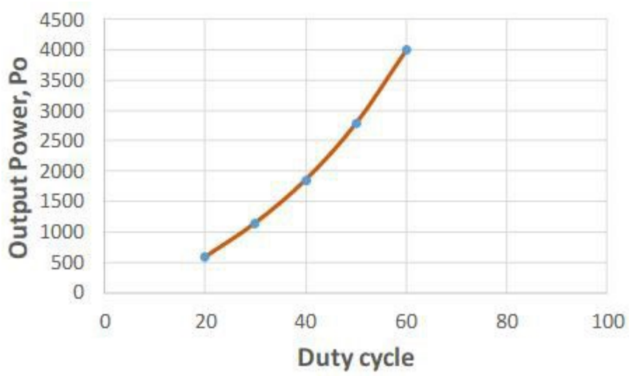

Fig. 7. Change in load power with duty cycle.

V. CONCLUSION

In this paper, an ac-ac inverter with boosting operation is proposed for induction heating application. The single stage ac-ac conversion reduces the power losses which are present in conventional two stage IH inverters. In the proposed ac-ac inverter an iron vessel is used as IH load. Output power is varied with duty cycle control. Independent control of output power for each half cycle of the supply voltage is possible in the proposed inverter. The inverter circuit is simulated for an output power of 4 kW. The inverter operation is verified through simulations in MATLAB/Simulink. Better source current profile is maintained for the full range of output power. With reduced component count, the proposed ac-ac inverter offers a compact, cost effective and high efficient solution for IH applications.

REFERENCES

[1] R. C. M. Gomes, M. A. Vitorino, D. A. Acevedo-Bueno, and M. B. d. R. Correˆa, "Multiphase resonant inverter with coupled coils for ac–ac induction heating application," *IEEE Transactions on Industry Applications*, vol. 56, no. 1, pp. 551–560, 2020.

[2] H.-P. Park and J.-H. Jung, "Load-adaptive modulation of a seriesresonant inverter for all-metal induction heating applications," *IEEE Transactions on Industrial Electronics*, vol. 65, no. 9, pp. 6983–6993, 2018.

[3] R. C. M. Gomes, M. A. Vitorino, D. A. Acevedo-Bueno, and M. B. d. R. Correˆa, "Three-phase ac–ac converter with diode rectifier for induction heating application with improved input current quality and coil modeling," *IEEE Transactions on Industry Applications*, vol. 57, no. 3, pp. 2673–2681, 2021.

[4] A. Trentin, P. Zanchetta, J. Clare, and P. Wheeler, "Automated optimal design of input filters for direct ac/ac matrix converters," *IEEE Transactions on Industrial Electronics*, vol. 59, no. 7, pp. 2811–2823, 2011.

[5] H. L. Li, A. P. Hu, and G. A. Covic, "A direct ac–ac converter for inductive power-transfer systems," *IEEE Transactions on Power Electronics*, vol. 27, no. 2, pp. 661–668, 2011.

[6] X. Lie, J. C. Clare, P. W. Wheeler, L. Empringham, and L. Yongdong, "Capacitor clamped multilevel matrix converter space vector modulation," *IEEE Transactions on industrial electronics*, vol. 59, no. 1, pp. 105–115, 2011.

[7] T. Wijekoon, C. Klumpner, P. Zanchetta, and P. W. Wheeler, "Implementation of a hybrid ac–ac direct power converter with unity voltage transfer," *IEEE Transactions on power electronics*, vol. 23, no. 4, pp. 1918–1926, 2008.

[8] H. Sarnago, O´ . Luc´ıa, M. Pe´rez-Tarragona, and J. M. Burd´ıo, "Dualoutput boost resonant full-bridge topology and its modulation strategies for high-performance induction heating applications," *IEEE Transactions on Industrial Electronics*, vol. 63, no. 6, pp. 3554–3561, 2016.

[9] S. Khatroth and P. Shunmugam, "Single-stage pulse frequency controlled ac–ac resonant converter for different material vessel induction cooking applications," *International Journal of Circuit Theory and Applications*, 2021.

[10] H. Sugimura, S.-P. Mun, S.-K. Kwon, T. Mishima, and M. Nakaoka, "High-frequency resonant matrix converter using one-chip reverse blocking igbt-based bidirectional switches for induction heating," in Proc. 2008 IEEE Power Electronics Specialists Conference, 2008, pp. 3960–3966.

[11] N. Nguyen-Quang, D. Stone, C. Bingham, and M. Foster, "Comparison of single-phase matrix converter and h-bridge converter for radio frequency induction heating," in Proc. 2007 European Conference on Power Electronics and Applications, 2007, pp. 1–9.

[12] N. A. Ahmed, "High-frequency soft-switching ac conversion circuit with dual-mode pwm/pdm control strategy for high-power ih applications," *IEEE transactions on industrial electronics*, vol. 58, no. 4, pp. 1440– 1448, 2010.

[13] H. Sarnago, A. Mediano, and O. Lucia, "High efficiency ac–ac power electronic converter applied to domestic induction heating," *IEEE transactions on Power Electronics*, vol. 27, no. 8, pp. 3676–3684, 2012.

[14] M. Ozturk and N. Altintas, "Multi-output ac–ac converter for domestic induction heating," *Electrical Engineering*, vol. 105, no. 1, pp. 297–316, 2023.

[15] H. Sarnago, O. Lucia, A. Mediano, and J. M. Burdio, "Direct ac– ac resonant boost converter for efficient domestic induction heating applications," *IEEE Transactions on Power Electronics*, vol. 29, no. 3, pp. 1128–1139, 2013.